

# Reducing the number of redundant pair-wise interactions in hydrodynamic meshless methods

Isaac Alonso Asensio<sup>★</sup> and Claudio Dalla Vecchia

*Instituto de Astrofísica de Canarias, C/Vía Láctea s/n, E-38205 La Laguna, Tenerife, Spain*

*Departamento de Astrofísica, Universidad de La Laguna, Av. Astrofísico Francisco Sánchez s/n, E-38206 La Laguna, Tenerife, Spain*

Accepted XXX. Received YYY; in original form ZZZ

## ABSTRACT

Widely used Lagrangian numerical codes that compute the physical interaction with neighbouring resolution elements (particles), duplicate the calculation of the interaction between pairs of particles. We developed an algorithm that reduces the number of redundant calculations. The algorithm makes use of a hash function to flag already computed interactions and eventual collisions. The result of the hashing is stored in two caches. Without limiting the cache memory usage, all duplicated calculations can be avoided, achieving the speed-up of a factor on two. We show that, limiting the cache size (in bits) to double the typical number of neighbouring particles, 70 per cent of the redundant calculations can be avoided, yielding a speed-up of almost 35 per cent.

**Key words:** methods: numerical

## 1 INTRODUCTION

A large number of numerical codes, employed in astrophysics to study the evolution of galaxies and the large-scale structure of the Universe, discretise the mass distribution into resolution elements (particles) of finite mass. Particles move in space according to the force exerted by the mass distribution in the simulated domain (e.g. pressure and gravity). Although algorithms have been developed to avoid the expensive calculation of particle-particle interactions over the whole domain, on small scales, particle-particle calculations are desired either to maintain high accuracy in the integration (e.g. gravitational forces) or for the local nature of the physical interaction (e.g. hydrodynamic forces). In order to conserve energy and momentum (and, eventually, mass), the interaction between two particles is generally antisymmetric by design of the algorithm.

One widely used example of an algorithm for solving the equations of hydrodynamics, and used in several fields of research to compute local pressure forces, is smoothed particle hydrodynamics (SPH; Lucy 1977; Gingold & Monaghan 1977). In the numerical implementation, the integration is performed as a sum of contributions from neighbouring particles. Several flavours of SPH have been developed (see, for example, the reviews of Rosswog 2009; Springel 2010a; Price 2012), in which the basic integration scheme is essentially the same. During a loop over all active particles, for each particle  $i$  its neighbours are searched, and their contribution to, e.g., the particle acceleration is computed and added,  $F_i = \sum_{j=1, N} F_{ij}$ . In the likely situation in which neighbouring particles are also active, the same pair-wise calculation is done twice for particles  $i$  and

$j$ , with the antisymmetry condition  $F_{ij} = -F_{ji}$ . This means that 50 per cent of the interactions that are computed among active particles are *redundant*, and skipping them would have a positive effect on the performance of the numerical code.

The same issue arises in other algorithm. The recently developed meshless hydrodynamic method by Lanson & Vila (2008a) has also been applied to astrophysical problems by Gaburov & Nittadori (2011); Hopkins (2015). In this case, the interaction among particles take the form of fluxes, computed after solving the Riemann problem at the interface between pairs of particles. As in SPH, tens of neighbouring particles are contributing to the calculation of the hydrodynamic quantities of each particle. The computation of fluxes is a time-expensive task, as there is no analytical solution to the Riemann problem, and an expensive, iterative procedure must be performed to converge to the solution. Therefore, decreasing the amount of Riemann problems to solve would have a noticeable effect on the performance of these methods.

Outside of fluid dynamics, the same issue can appear when computing the gravitational forces among particles using the direct summation method. Even in the cases where the long-range forces are approximated as a multipole expansion, for short-range forces, a considerable number of direct summations is performed (Barnes & Hut 1986). Likewise, cell-cell interactions within the Fast Multipole Method could lead to duplicated calculations (Greengard & Rokhlin 1997).

In this work, we aim to reduce the amount of redundant computations whilst keeping small memory footprint and computational overhead. We present a novel algorithm which makes use of caches to store the information of already computed interactions. In the test applications in this work, this algorithm can avoid  $\sim 70$  per cent of the redundant computations, which translates to a theoretical speed

<sup>★</sup> E-mail: isaacaa@iac.es (IAA)

up (as defined in appendix A) of 35 per cent. The parameters of the algorithm can be tuned to increase its performance at the cost of an increased memory footprint.

The problem of redundant calculations is detailed in section 2. In section 3, we describe the novel algorithm to reduce the amount of duplicated computations. In section 4, we test the algorithm in idealised cases and cosmological simulations.

## 2 REDUNDANT PAIR-WISE INTERACTIONS

As a general case, we can write the time derivative of a variable,  $u$ , of particle,  $i$ , as the sum of the different contributions of neighbouring particles,  $j \in \mathbb{S}_i$ ,

$$\frac{du_i}{dt} = \sum_{j \in \mathbb{S}_i} F_{ij}, \quad (1)$$

where the term  $F_{ij}$  are the contributions to the derivative of variable  $u_i$  from particle  $j$ . Furthermore, we assume antisymmetry,  $F_{ij} = -F_{ji}$ , as it keeps the algorithm conservative.

The specific functional form of the contribution will depend on the problem and scheme at hand. For example, the contributions can be the Van der Waals forces between hydrogen atoms pairs or the gravitational force between two particles, among others. In our particular case, these contributions are hydrodynamical forces between particles, following Lanson & Vila (2008a); Gaburov & Nitadori (2011); Hopkins (2015).

If each particle has  $N_{\text{NGB}}$  neighbouring particles, and we have  $N$  particles in total, ideally we would need  $\frac{1}{2}N \times N_{\text{NGB}}$  evaluations of the contribution,  $F$ , thanks to antisymmetry.

However, it is typical in most implementations of Lagrangian codes to proceed as follows: 1) a loop over all particles is performed; 2) within the loop, for each particle  $i$ , the neighbouring particles are gathered; 3) all the neighbouring particles' contributions are computed and added to particle  $i$ . In this way, each contribution is computed *twice*: for particle  $i$  ( $F_{ij}$ ) and for particle  $j$  ( $F_{ji}$ ), when the two particles are reached. We will denote this as the *gather* approach.

In order to avoid redundant calculations, particles must always keep information about its neighbours, such that, for each pair  $(i, j)$ , one could check if  $F_{ji}$  ( $F_{ij}$ ) has already been computed, and only if not, compute  $F_{ij}$  ( $F_{ji}$ ). In both cases, the contribution is computed only once and added to both particles. This would be the *scatter* approach.

Both implementations are exactly the same from a numerical point of view, as they lead to the same solution. However, from the computational point of view they are very different. On one hand, the gather approach is easier to implement and allows for more flexibility: this implementation is completely agnostic to the total number of particles, and the geometry formed by them. On the other hand, the scatter approach requires less evaluations of  $F$ , at the cost of a substantial increase of the required memory per particle, as the list of neighbours have to be stored together with the information on which contributions have been already calculated.

## 3 ALGORITHM TO REDUCE DUPLICATED INTERACTIONS

In this section, we first describe in detail the scatter approach, and highlight its drawbacks and advantages. Then, we will introduce the new cached contributions algorithm, which mix the scatter and

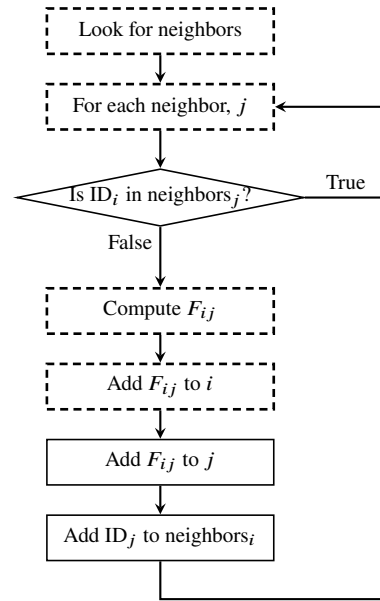


**Figure 1.** Naive approach to avoid computing all the redundant contributions. This requires for each particle an array of all the neighbouring particle IDs, which substantially increases the memory footprint of the particles. For clarity, we omit the outer loop over all the particles.

gather approaches to reduce the amount of duplicated computations substantially and with minimal memory requirements.

### 3.1 Scatter method

A simple scatter algorithm is represented in figure 1. The method needs the allocation of an array of size  $N_{\text{NGB}}$ , storing the particles IDs of the neighbours whose contribution have been computed.

Each time that a contribution  $F_{ij}$  is to be computed, whether  $i$  is in the neighbours array of  $j$  is checked. If true, the contribution has already been computed (by particle  $j$ , and added to both  $i$  and  $j$ ) and can be skipped. Otherwise,  $F_{ij}$  is evaluated, added to both particles, and the ID of particle  $j$  is added to the neighbours array of  $i$ .

This simple implementation increases by a large factor the memory footprint per particle. If, as in typical hydrodynamic simulations,  $N_{\text{NGB}} \sim 50$ , then the required memory per particle would increase by 200 bytes (if 32 bits variables are used). The method may not be using each array of neighbours at its full capacity. For example, for each particle in the main loop, one needs to store only the neighbours that have not interacted earlier in the loop. It is also worth noticing that this approach only avoids computing 100 per cent of the redundant contributions if  $N_{\text{NGB}}$  is smaller than or equal to the size of the allocated array for all particles. If the number of neighbours is not constant in space and/or time, this algorithm can be highly inefficient because the neighbours array may be needed to be dynamically allocated for each particle during the simulation.

It is important to note that an increase of the memory per particle does not only decrease the maximum number of particles that fit in the memory of a given system, but also increases substantially the latency, as less particles can be fitted into the CPU cache. This, in turn, can slow down considerably the calculation and create even more severe latency problems in distributed memory machines. This approach, although simple to implement and test, has impor-

tant efficiency drawbacks, and has not been implemented in popular hydrodynamic codes (to our best knowledge).

### 3.2 Cached contribution algorithm

The naive scatter approach explained above has two serious drawbacks, namely, large memory footprint and strong dependency on  $N_{\text{NGB}}$ . The algorithm proposed in this work, and detailed in this section, aims to minimise the drawbacks at the cost of allowing for a small fraction of the redundant computations to be done. Concerning the memory usage, instead of saving an array of neighbours of size  $N_{\text{NGB}}$ , just two scalars are saved: a contribution and a collision cache. Furthermore, a hash function is used to convert the neighbouring particle's ID into an integer indicating which bit of the cache corresponds to that neighbour.<sup>1</sup>

The algorithm is detailed in figure 2. We use the notation  $\text{cache}_i[\text{index}_j]$  to refer to the bit in the  $\text{index}_j$  position of the cache of particle  $i$ . The outer loop, which runs over all particles, has been omitted for clarity. The algorithm can be split into two blocks. In the upper block, just after the neighbours search, the cache is built: for each neighbour, its cache position is computed with the hash function, and the corresponding bit in the cache is set equal to 1. In the case that another neighbour has the same cache position, a collision is flagged by setting the corresponding bit to 1 in the collision cache. In this case, the contribution will be recomputed. If neighbour  $j$  has already computed  $F_{ji}$ , and the contribution has been added to particle  $i$ , there is no need of storing  $j$  in the cache, eventually saving space for other neighbours, and reducing the probability of collision.

After the cache has been built, the standard procedure to compute  $F$  follows, but with two checks: 1) if a neighbour  $j$  has already computed the contribution and added it to particle  $i$ , the redundant computation is skipped; 2) the contribution is added to neighbour  $j$  (scatter method) only if it has not been computed before for that particle, and there is no collision flagged in the cache of particle  $i$ . As long as we are not in case 1), the flux contribution is always added to particle  $i$  (gather method).

In summary, there are three possible outcomes for the particles pair  $(i, j)$ :

- (i) the computation of the flux is redundant and there is no collision: it can be skipped;
- (ii) there is a collision either in the cache of  $i$  or  $j$ ; the flux has to be (re)computed;
- (iii) there are no collisions and the flux is computed for the first time.

Ideally, one wants to minimise the second case, which in turn decreases the amount of recomputed contributions. In appendix A, we study in detail how the different scenarios and parameters change the performance of the algorithm in idealised cases. As first indication, we recommend using a cache size of  $\sim 2N_{\text{NGB}}$  bits to obtain good performance with low memory footprint.

## 4 RESULTS

We have implemented the algorithm within a modified version of PKDGRAV3 (Potter et al. 2017) which includes meshless hydro-

<sup>1</sup> The ID is a generic identifier of a particle, but it does not have to be unique, as long as it can be hashed into the cache. For example, it can be the memory address of the particle.

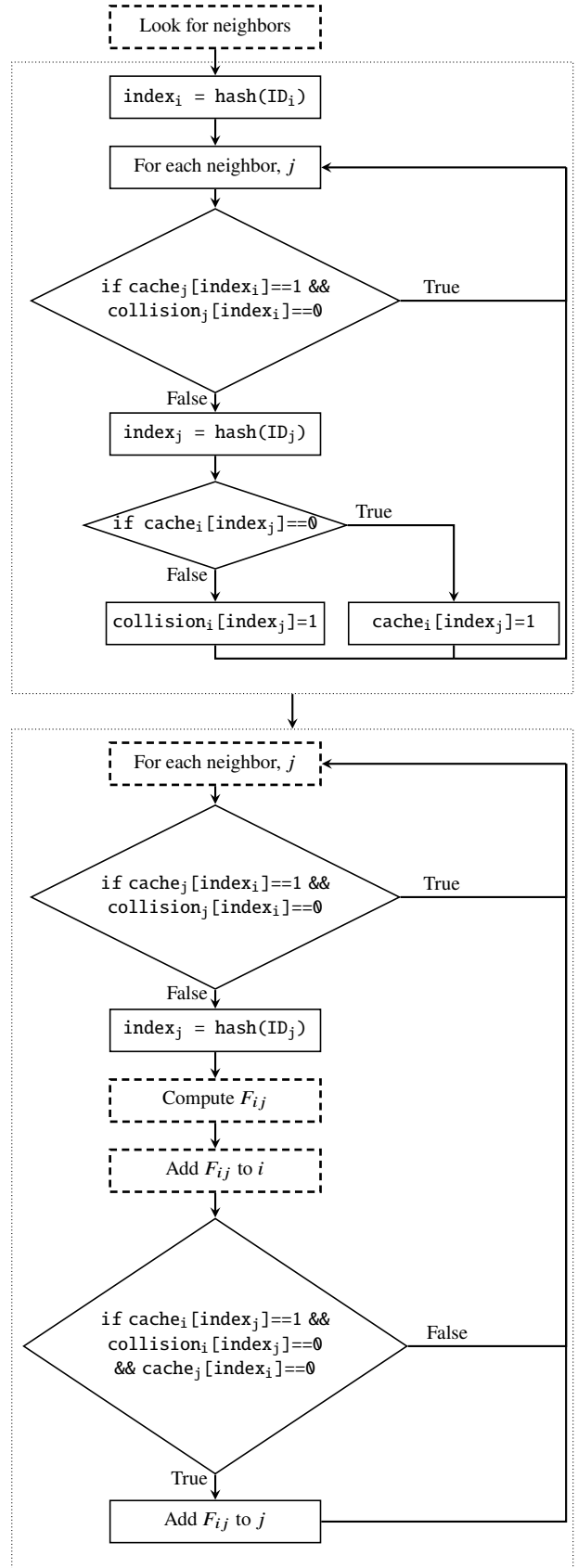


**Figure 2.** Algorithm to reduce the number of redundant interactions. The algorithm is divided in two blocks (dotted lines), and the nodes with dashed lines are those which are performed in a typical implementation where all the redundant contributions are computed. For clarity, we omit the outer loop over all the particles.

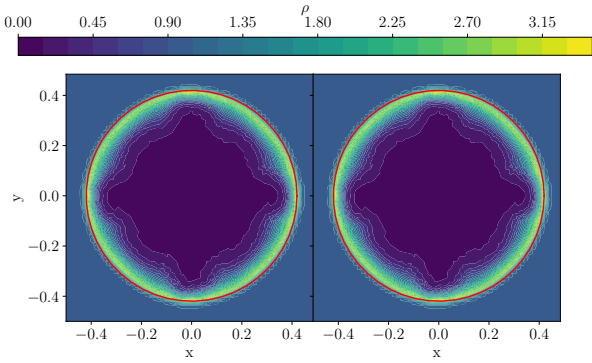


**Figure 3.** Projected density maps on a slice through the centre of the Sedov explosion at  $t=0.8$ . *Left panel:* cached run employing the novel algorithm to reduce the number of flux computations. *Right panel:* standard run, in which all redundant contributions are computed. The red line marks the analytic prediction at the same time. The density maps are indistinguishable.

dynamics similar to [Lanson & Vila \(2008a,b\)](#); [Gaburov & Nitoro \(2011\)](#); [Hopkins \(2015\)](#), with a time step hierarchy following [Springel \(2010b\)](#). The code in question will be described elsewhere, as the exact hydrodynamic scheme is of no special importance in this work.

For the following simulation tests, the cache size has been set to 64 bits (`uint64_t`), and the number of neighbours to  $N_{\text{NGB}} = 32$ . However, the number of neighbours can vary as we iteratively solve the equality:

$$\frac{4\pi}{3} \omega_i h_i^3 = N_{\text{NGB}}, \quad (2)$$

where  $h_i$  is the smoothing length and  $\omega_i = \sum_j W_{ij}(h_i)$ , an approximation of the local number density of particles. This is a standard procedure, explained in detail in, e.g. [Rosswog \(2009\)](#). Although the hydrodynamic solver we have implemented works as well with a fixed number of neighbours, we discuss here this less favourable approach to highlight the performance improvement other hydrodynamic solvers can achieve (e.g., smoothed particle hydrodynamics).

In the next section, we assess the performance of the code in a standard test case for hydrodynamics solvers, the Sedov explosion. This will help us to illustrate how the algorithm ensure the conservation of the hydrodynamic quantities. Then, in section 4.2, we will use this algorithm in a more challenging and interesting case, a cosmological, hydrodynamic simulation. We will study the theoretical speed up (i.e., the ratio between avoided and computed plus avoided fluxes, as described in appendix A) achieved in the tests.

#### 4.1 Sedov explosion

In this section we study a point explosion, with an energy input much greater than the background energy of the medium. This test will serve as a first case illustrative application of the algorithm.

We set up the particles in a Cartesian grid with  $N = 64^3$  particles in a box of size  $L = 1$ . We assign their masses such that the density is unity in the domain. The background internal energy is  $10^{-5}$  and for the central particle a internal energy of 1 is added. We let the system evolve until  $t = 1$ . Hereafter, we will denote the runs with and without the algorithm as *cached* and *standard*, respectively.

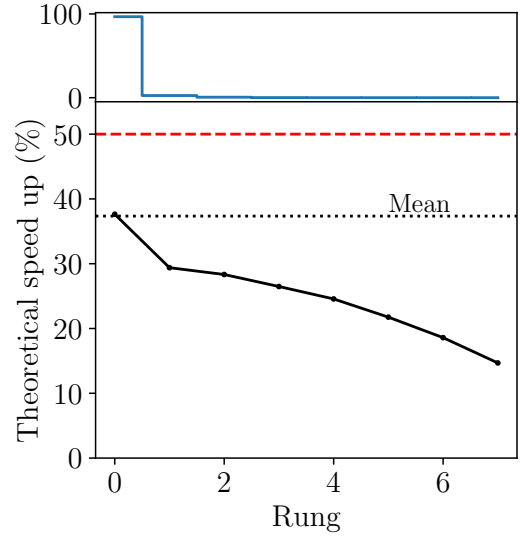


**Figure 4.** *Bottom panel:* theoretical speed up (i.e., ratio of avoided over avoided+computed fluxes) as a function of the particle rung for the Sedov explosion. The algorithm performs poorly for particles on the smallest timestep, as they are distributed in a thin shell. The maximum achievable theoretical speed up is shown as a red, dashed line. *Top panel:* Percentage of fluxes computed in a given rung. The rungs with the lowest performance are those with the smallest number of interactions, thus they do not affect the mean performance (dotted line).

Given that the underlying hydrodynamic scheme is conservative, so it must be when we apply the new algorithm. We have checked that this is the case for the Sedov explosion. We find that applying the new algorithm does not degrade the solution or break the conservation of physical quantities, the latter being exact at machine precision. Just to illustrate this qualitatively, we show in figure 3 projected density maps on a thin slice centred on the origin for the standard and cached runs (right and left panels, respectively). The maps are indistinguishable.

We can now investigate what fraction of calculations has been avoided. For this case, we have calculated a theoretical speed up of  $\sim 37$  per cent, similar to the expectation value in appendix A. This means that more than 75 per cent of the redundant contributions have been skipped.

In both runs, we have used individual particle time steps (see more details in appendix B), where the allowed time steps are power of two divisions of a global timestep:  $\Delta t_i = 2^{-r_i} \Delta t$ . We refer to the integer  $r_i$  as the rung of a particle. In the particular case of the Sedov explosion, we expect the algorithm to perform poorly for particles with the smallest timestep ( $r \gg 1$ ,  $\Delta t_i \ll \Delta t$ ), as they are distributed in a thin, spherical shell around the centre of the explosion, thus only a handful of their neighbours will reside on the same time step rung and can take advantage of the algorithm. We show this in the bottom panel of figure 4, where the theoretical speed up is shown for each rung. The general trend is a lower speed up towards smaller time steps. However, as the amount of particles of high rung is small compared to the total (figure 4, top panel), the global speed up is only marginally affected (dotted line in the bottom panel).

#### 4.2 Cosmological application

Although the algorithm presented here can be applied to a wide variety of problems, it was devised to be used in cosmological, hy-

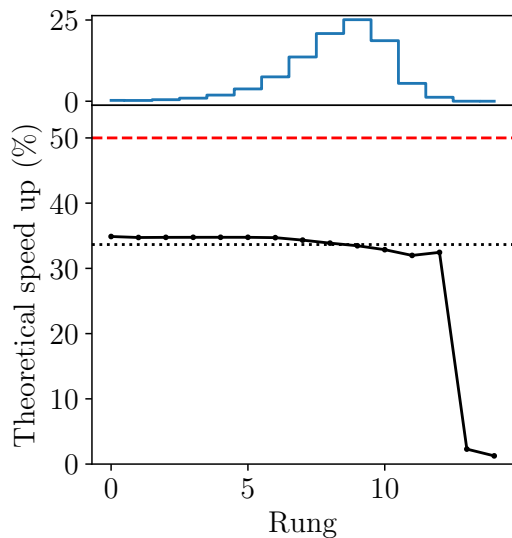


**Figure 5.** *Bottom panel:* theoretical speed up (i.e., ratio of avoided over the sum of avoided and computed fluxes) as a function of the particle rung for a cosmological simulation of box size  $L = 20$  Mpc. The maximum achievable theoretical speed up is shown as a red, dashed line. *Top panel:* Percentage of fluxes computed in a given rung.

drodynamic simulations. In this section we assess the performance improvement for this case.

We generated initial conditions for a cosmological box of size  $L = 20$  Mpc, with  $N = 2 \times 128^3$  particles (dark matter and gas), at  $z = 49$  using 2LPTic (Crocco et al. 2006). We ran two simulations to  $z = 0$  with identical code configuration and parameters.

The theoretical speed up in the cached run is 33.6 per cent, in good agreement with the above figures. As in the Sedov test, we can study the performance depending on the time step rung of the particle. This is shown in figure 5. As expected, the most active particles, residing in the centre of halos, do not take full advantage of the algorithm, as either a small fraction of their neighbours is in the same rung or their number of neighbours exceed the cache size. However, this only marginally affects the mean behaviour (dotted line), because they only account for a small fraction of the computed interactions.

The cosmological simulations are useful for studying how the algorithm behaves in two different regimes: almost uniform matter (particle) density at  $z = 49$ , where all particles are expected to have a similar number of neighbours of the same rung; and highly clustered regions at  $z = 0$ , where particles are distributed over several rungs and their number of neighbours can largely vary. We show the cache occupancy and collision statistics in figure 6. We show in the top panels the histograms of the cache occupancy (left) and collision rate (right). When particles are highly clustered, both occupancy and collision rates show a tail towards higher values. This is caused by particles that have a number of neighbours greater than  $N_{\text{NGB}}$ . However, the number of particles in the tail is negligible compared to the total, and the algorithm performance is rather uniform in space and time.

On the bottom left panel, the 2D contours of the previous quantities show that, regardless of the tail at  $z = 0$ , the mean behaviour is similar. Lastly, in the bottom right panel, the histogram of the theoretical speed up per particle is shown. It is evident that the algorithm performs better in the absence of clustering, but the difference is not

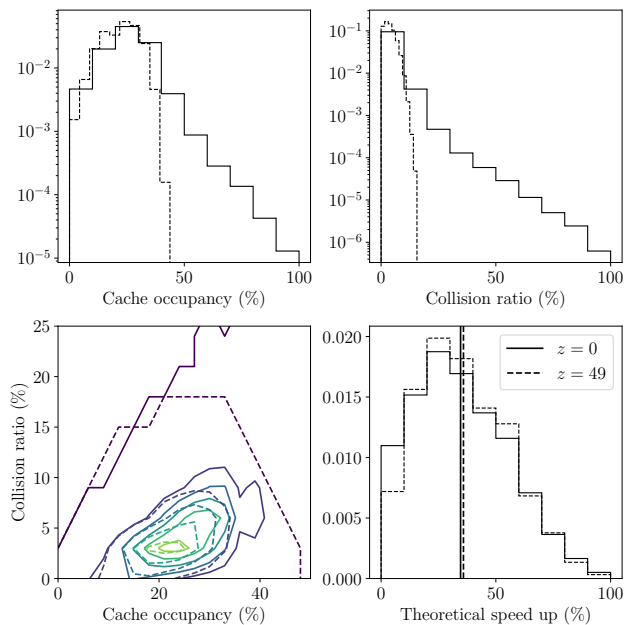


**Figure 6.** Summary statistics for the cosmological simulation test at  $z = 0$  (solid lines) and  $z = 49$  (dashed lines). Top panels show the distribution of cache occupancy (left panel) and collision ratio (right panel). The 2D contours of those are shown in the lower left panel. The histogram of the theoretical speed up per particle is shown in the lower right panel, with the mean values denoted as vertical lines.

remarkable. The theoretical speed up is 34.6 and 35.8 per cent for  $z = 0, 49$ , respectively. Thus, the effect of the clustering is even less important when measuring the mean performance of the algorithm.

## 5 CONCLUSIONS

We have developed a new algorithm (section 3.2, figure 2) to reduce the amount of redundant flux computations, a problem typical of Lagrangian integration methods, such as SPH. This algorithm, however, can be used in any other pair-wise interaction that follows the general form shown in equation (1). An example apart from hydrodynamic computations would be the solution of the Poisson equation using the direct summation method, which is typically done for close particle-particle interactions in tree codes, or the pair-wise interactions in molecular dynamics codes.

This algorithm has a very low memory footprint per particle (16 bytes per particle in our implementation), but can remarkably avoid  $\sim 70\%$  of the redundant interactions, at a negligible amount of computational cost. The key idea is to store a cache of computed interactions, together with a collision cache which marks which elements of the former can be trusted. Then, the particle IDs are hashed into the cache. If the particle contribution was already computed and there are no collisions in either caches, the calculation can be skipped.

This algorithm does not modify the underlying hydrodynamics solver, thus produces exactly the same physical results but at a lower cost. This has been tested in the Sedov explosion, where the solution has been shown to be unmodified when applying the novel algorithm (figure 3), and the conservation properties of the method have been confirmed to be untouched.

Also it has been applied in a cosmological context, where a

theoretical speed up of 33% was obtained. The dependence of the algorithm performance on the timestep of the particles (figure 5) and clustering (figure 6) was analysed, and we found that the algorithm does not drastically reduce its performance in most cases.

The presented algorithm is very versatile, as the only parameters required is the cache size. However, it can have some other dependencies in the parameters of the simulation, such as the number of neighbours, particle number, dimensionality,... These were thoroughly studied, and are presented in appendix A. Furthermore, we also detail some parts of our specific implementation in appendix B.

All in all, the algorithm presented here is an easy to implement addition to meshless codes, which may increase their performance substantially. Furthermore, it presents great potential to be applied in other fields of (Astro-)Physics that require the evaluation of pairwise interactions.

## ACKNOWLEDGEMENTS

The author thankfully acknowledges the technical expertise and assistance provided by the Spanish Supercomputing Network (Red Española de Supercomputación, RES), as well as the RES computational resources used in this work: the LaPalma supercomputer, located at the Instituto de Astrofísica de Canarias (IAC granted time), and the MareNostrum supercomputer, located at the Barcelona Supercomputing Center (time awarded to proposal AECT-2020-2-0003). IAA and CDV are supported by the Ministerio de Ciencia, Innovación y Universidades (MCIU/FEDER) under research grant PGC2018-094975-C22. CDV acknowledges the support of MCIU through grant RYC-2015-18078.

## DATA AVAILABILITY

An implementation of the novel algorithm, written in Python, can be found in <https://github.com/Isaac-a95/CachedFluxes>. This script also generates the figures in appendix A. The rest of the data underlying the article will be shared on reasonable request to the corresponding author.

## REFERENCES

- Barnes J., Hut P., 1986, *Nature*, 324, 446  
 Croce M., Puelbas S., Scoccimarro R., 2006, *Monthly Notices of the Royal Astronomical Society*, 373, 369  
 Gaburov E., Nitadori K., 2011, *Monthly Notices of the Royal Astronomical Society*, 414, 129  
 Gingold R. A., Monaghan J. J., 1977, *Monthly Notices of the Royal Astronomical Society*, 181, 375  
 Greengard L., Rokhlin V., 1997, *Journal of Computational Physics*, 135, 280  
 Hopkins P. F., 2015, *Monthly Notices of the Royal Astronomical Society*, 450, 53  
 Lanson N., Vila J.-P., 2008a, *SIAM Journal on Numerical Analysis*, 46, 1912  
 Lanson N., Vila J.-P., 2008b, *SIAM Journal on Numerical Analysis*, 46, 1935  
 Lucy L. B., 1977, *The Astronomical Journal*, 82, 1013  
 Potter D., Stadel J., Teyssier R., 2017, *Computational Astrophysics and Cosmology*, 4, 2  
 Price D. J., 2012, *Journal of Computational Physics*, 231, 759  
 Rosswog S., 2009, *Advances in the Free-Lagrange Method Including Contributions on Adaptive Gridding and the Smooth Particle Hydrodynamics Method*, pp 239–247

Springel V., 2005, *Monthly Notices of the Royal Astronomical Society*, 364, 1105

Springel V., 2010a, *Annual Review of Astronomy and Astrophysics*, 48, 391  
 Springel V., 2010b, *Monthly Notices of the Royal Astronomical Society*, 401, 791

## APPENDIX A: DEPENDENCE ON PARAMETERS AND CASE

We describe here the tests performed to quantify the performance of the algorithm for different particles and parameters configurations. To study the algorithm in a controlled way, such that no information about the underlying code (e.g. the hydrodynamic scheme) is of relevance, we have written a Python module which implements the algorithm described in this work. This can be found at <https://github.com/Isaac-a95/CachedFluxes>.

The script does not implement the calculation of any specific physical quantity (e.g., fluxes, gravitational forces, etc.). Rather, by counting the redundant computations, it outputs the theoretical speed up, defined as the ratio of avoided calculation over the total number of particle-particle interactions. If the computational time in the underlying code is dominated by the computation of the particle-particle interactions, this will be approximately the true speed up.

Unless otherwise stated, the default parameters for the following tests are: total number of particles,  $N = 10000$ , cache size of 64 bits and number of neighbours,  $N_{\text{NGB}} = 32$ .

### A1 Dependence on hash function

The hash function is in charge of converting a particle ID, or other particle property, into a cache position. In order to minimise the collision rate, we require that the hash function distributes regularly input IDs into the cache space, given that they do not follow any particular order (this last point will be discussed below). The simplest hash function that has this property is the modulo operator. Furthermore, given that the cache bit size is a power of two, this operation can be heavily optimised by the compiler using bit-wise arithmetic. In this work we have always been using the modulo operator, and we postponed the detailed comparison of different hash function as a future project. However, we expect little to no performance differences when changing hash function, provided that the function meets the minimal requirements stated above.

### A2 Dependence on order of execution

The precise performance of this method may depend on the order of execution of the outer particle loop. To simply illustrate this, let us suppose that  $N$  particles are distributed in one dimension (this algorithm is agnostic to the dimensionality of the problem). The particle outer loop could be performed in two ways: according to the particle spatial ordering (left-to-right or right-to-left), or according to their (aleatory) ordering in memory.

In the first case, the probability of having previously computed a flux is  $\mathcal{P}_{j \rightarrow i} = \frac{1}{2}$ , therefore one would expect  $N_{\text{NGB}}/2$  elements per cache.<sup>2</sup> Given the default configuration, in which the cache size

<sup>2</sup> For sake of simplicity, we do not consider particles close to the boundaries of the domain.

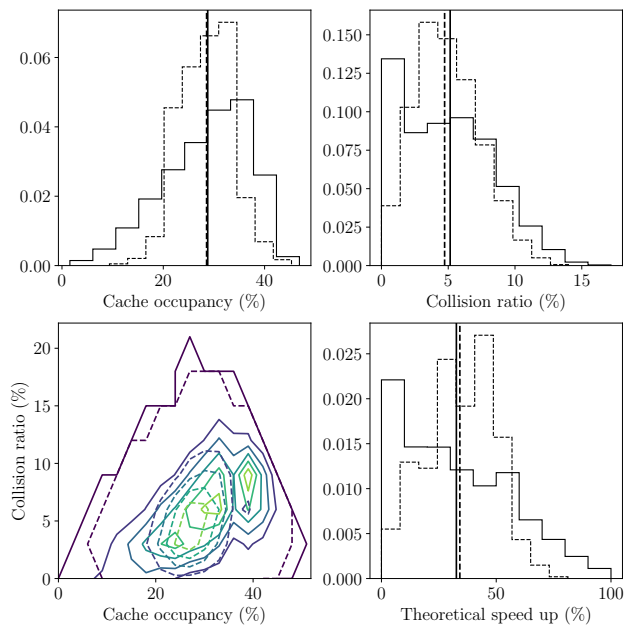


**Figure A1.** Statistics for the ordered (dashed lines) and unordered (solid lines) execution of the hydrodynamic loop. Top left and right panels show the histograms of the cache occupancy and collision ratio, respectively. The 2D contours of those are shown in the bottom left panel. The histogram of the theoretical speed up per particle is shown in the bottom right panel.

in bits is twice  $N_{\text{NGB}}$ , the cache occupancy will be small and almost constant, of about 25 per cent.

In the second case, the probability will depend on the particle position in the loop. For particle  $i$ , the probability that the flux has been previously computed is  $\mathcal{P}_{j \rightarrow i} = i/N$ . This implies a much wider cache occupancy distribution. However, the average probability will be  $\langle \mathcal{P}_{j \rightarrow i} \rangle = \frac{1}{2}$ , so that the order of execution will only have marginal effects on the performance gain of the method.

To illustrate this, we have run the algorithm with ordered (dashed line) and unordered (solid line) particle distributions. The result is shown in figure A1. The cache occupancy is shown in the top left panel. The distributions are different, but their average are very similar: 28.4 and 28.7 per cent for ordered and unordered particles, respectively. The same is found for the collision ratio (top right panel), with mean collision rates of 4.8 and 5.1 per cent, and theoretical speed up per particle, 34.1 and 32.8 per cent, shown in the bottom right panel. In summary, the change of the order of execution has only marginal effects on the mean behaviour of the algorithm presented in this work.

### A3 Dependence on particle IDs

In this work, we have used the particle IDs as input for the hash function, assuming that the IDs do not follow a preferential spatial ordering within the simulated volume. This is a requirement for the particular choice of hash function. In any case, whatever the input of the hash function is, it should not carry any information on the spatial distribution of particles in order to avoid to introduce any bias due to the locality of the computation.

As an example, we discuss the possible drawbacks of an initial (quasi) Cartesian mesh distribution of particles, a typical distribution for the initial conditions of cosmological simulations. Given a

**Table A1.** Dependence on the dimensionality of the problem, with the default configuration.

Dimensions	1	2	3
Theoretical speed up	33.9%	33.1%	32.8%

**Table A2.** Dependence on the number of particles, with the default configuration.

$N$	100	1000	10000
Theoretical speed up	35.7%	32.2%	32.5%

cubic volume of side  $L$  with  $N_L$  particles per side, each particle would lie in a position (close to)  $(iL/N_L, jL/N_L, kL/N_L)$ , where  $i, j, k \in [0, N_L]$ . A natural choice for assigning unique IDs is to use the integers  $i + jN_L + kN_L^2$ . This implies that, if  $N_L$  is a multiple or divisor of the cache size, particles in adjacent planes, but aligned along the orthogonal axis, will generate collisions in the cache, as the hash function will return the same bit position. This can greatly decrease the performance of the method.

The simplest solution is to randomise the assignment of IDs to the particles. As long as the particle IDs are not needed to be correlated with spatial information (that does not seem to be the requirement in the majority of astrophysical simulations), this can be done without any loss of information. In the case the IDs are used to carry information on the initial conditions, a different choice of hash function should be made.

### A4 Dependence on dimensionality

The algorithm is completely agnostic to the number of dimensions of the problem. To verify this, we changed the dimension of the problem from 1 to 3. In table A1, we show the theoretical speed up for each choice of dimensions, using the default parameters. As expected, there is no trend with the number of dimensions, and the negligible differences can be attributed to random variations from run to run.

### A5 Dependence on number of particles

The total number of particles should not influence the performance of the algorithm, because the algorithm itself depends only on the (local) number of neighbours, by construction.

To illustrate this, we ran the algorithm with  $N = 100, 1000$  and 10000 particles. As we randomise the IDs, the performance for  $N = 100$  will have more variance compared to higher  $N$ . To correct this, and calculate a meaningful average performance, we do average the results of 100, 10, 1 runs for  $N = 100, 1000, 10000$ , respectively.

In table A2, we show the average theoretical speedup in each case. As expected, there is no clear trend with particle number, thus the algorithm can be safely used even when only a few particle contributions are computed. Note, however, that this few particle must be neighbours with each other in order to take advantage of this algorithm.

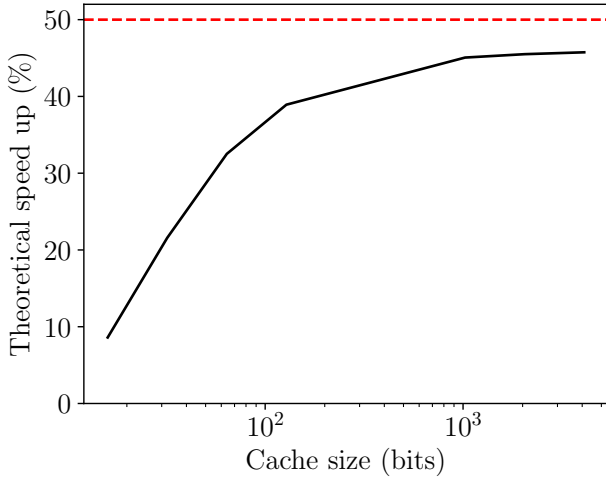


**Figure A2.** Dependence of the algorithm performance on the cache size, fixing the number of neighbours. The red line marks the maximum theoretical speed up.

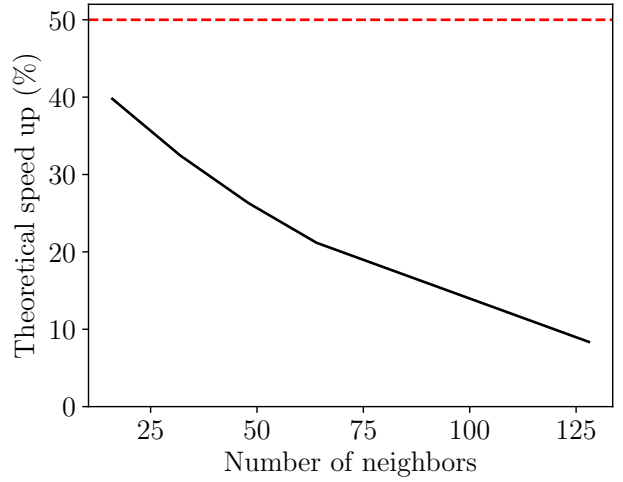


**Figure A3.** Dependence of the algorithm performance on the number of neighbours for a fixed cache size. The red, dashed line marks the maximum theoretical speed up.

#### A6 Dependence on cache size

It is trivial to show that the larger the cache, the less probable a collision is. In the limit of cache size approaching the total number of particles, all collisions are avoided, as the hash function we employ would return a unique bit position per particle. On the other hand, increasing the cache size can become prohibitive in terms of memory usage.

As an illustrative example, we have run the algorithm varying the cache size from 16 to 4096 bits in power of two steps. The theoretical speed up is shown in figure A2. It saturates at around  $\sim 45$  per cent because particles are not required to be mutual neighbours in our implementation of the test code. However, in SPH, this is forced in order to conserve the total energy and momentum, and one can expect the speed up to reach 50 per cent. In any case, using such big caches is not practical.

A speed up of 30 per cent can be achieved with a cache of size  $2N_{\text{NGB}}$  bits or slightly larger. However, even smaller cache size still lead to a good performance of the algorithm, with about 20 per cent speed up achieved with a cache size equal to the number of neighbours.

#### A7 Dependence on number of neighbours

Together with the cache size, the number of neighbours is key to the performance of the algorithm. The lower the number of neighbours, the less the cache requests and, potentially, collisions. To quantify this effect, we ran the algorithm increasing the number of neighbours from 16 to 128, fixing the cache size to 64 bits.

The theoretical speed up is shown in figure A3. As expected, the performance decreases with increasing number of neighbours. However, even when the cache size is half  $N_{\text{NGB}}$ , the speed up is still above 10%. This is of particular importance in cases where the number of neighbours is not constant, but rather an estimate of the local (number) density, as in equation 2.

We can infer from the previous figures that the important parameter to control the theoretical speed up is a combination of the cache size and  $N_{\text{NGB}}$ . In figure A4 we show the speed up when we fix the ratio of cache size to  $N_{\text{NGB}}$  to 4 (dashed), 2 (solid), 1 (dot-dashed) and 1/2 (dotted), 1

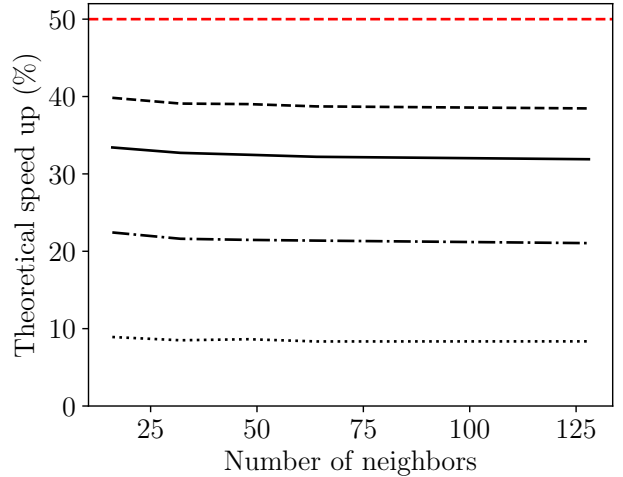


**Figure A4.** Dependence of the algorithm performance on the number of neighbours, fixing the ratio of the cache size over  $N_{\text{NGB}}$  to 4 (dashed), 2 (solid), 1 (dot-dashed) and 1/2 (dotted). The red, dashed line marks the maximum theoretical speed up.

(dot-dashed) and 1/2 (dotted). Fixing this ratio produces a nearly constant performance independently of the value of  $N_{\text{NGB}}$ . We therefore suggest the use of a cache of size  $\geq 2N_{\text{NGB}}$ , but recall that, if the number of neighbour widely oscillate around the average, a small performance decrease has to be expected. If only a negligible number of particles are filling the high  $N_{\text{NGB}}$  tail, we saw in section 4.2 that the performance decrease is also negligible.

## APPENDIX B: IMPLEMENTATION CONSIDERATIONS

In order to keep the description of the algorithm general, we have avoided to discuss the details of the implementation, that can differ from code to code. In this appendix, we describe the implementation

choices for this work, which, although not part of the algorithm itself, they may change its performance.

### B1 Time stepping

In the code used for this work, a power-of-two time step hierarchy is used, such that particles with large rung (short time step) require more frequent updates than particles on lower rungs. Particles that need an update at a given simulation time (they are at the end of their time steps, independently of the length of the time step) are usually denoted as active. Conversely, particles that are not synchronised are denoted as inactive. The time step hierarchy method is further explained in, e.g., [Springel \(2005, 2010b\)](#).

In order to maintain conservation of energy and momentum, when computing the interaction between particles, the smallest of the two time steps is used for the integration. Moreover, when computing the interaction between active and inactive particles, the contribution is always added to the inactive particle. In this case, there is no redundant computation (the inactive particle does not compute its contribution), and the inactive particle does not need to be added to the cache. Therefore, for particles on individual time steps, the maximum theoretical speed up is lower than 50 per cent, because all interactions with inactive particles are not counted. On the other hand, there would be more space available in the cache, reducing the number of collisions. In the general case, where the time step is set by local properties of the fluid, one should expect that most of neighbouring particles share the same time step and a small impact of the hierarchical time stepping on the performance of the algorithm.

### B2 Parallelisation

There are plenty of strategies to take advantage of multiple CPUs, both in distributed and shared memory or hybrid machines. It is not the purpose of this work to assess how this algorithm may be parallelised. In fact, the implementation used in this work is serial, and applied only to particles assigned to the same core. Of course, this can decrease the performance of the algorithm. To assess how much the overall performance is degraded, we have run a single step (at  $z = 49$ ) of the cosmological, hydrodynamic simulation with different numbers of cores. In the results presented in section 4.2, we used 48 cores. Here, we will decrease this value (and, conversely, increase the number of particles per core) down to just 2 cores. The theoretical speed up is shown in figure B1.

For a fixed problem size, increasing the number of cores results in a decrease of the performance. However, the decrease is merely  $\sim 1$  per cent when varying the number of cores from 2 to 48. For the run with 48 cores, the number of particles per core is about 40,000, which is way lower of that in typical cosmological simulations. We are therefore confident that parallelising the algorithm would not provide better performance.

This paper has been typeset from a  $\text{\TeX}/\text{\LaTeX}$  file prepared by the author.

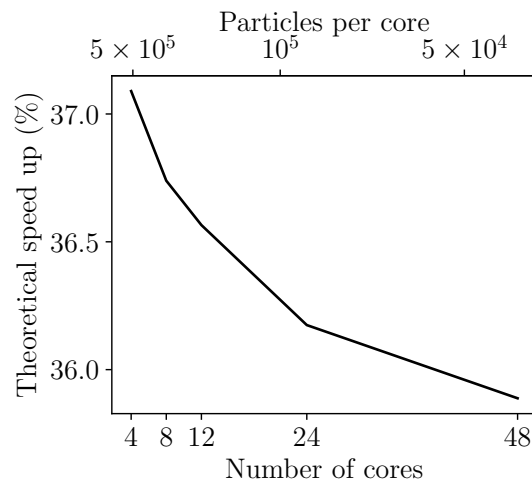


**Figure B1.** Strong scaling of the implementation. We fix the problem size (see section 4.2), and change the number of cores. Only a change of 1 per cent in the performance is seen when changing the number of cores from 2 to 48.